Published in final edited form as:
J Mol Cell Cardiol. 2010 October ; 49(4): 683–692. doi:10.1016/j.yjmcc.2010.06.003.

SGLT1, a Novel Cardiac Glucose Transporter, Mediates Increased Glucose Uptake in *PRKAG2* Cardiomyopathy

Sanjay K. Banerjee[a], **David W. Wang**[a], **Rodrigo Alzamora**[b], **Xueyin N. Huang**[a], **Núria M. Pastor-Soler**[b], **Kenneth R. Hallows**[b], **Kenneth R. McGaffin**[a], and **Ferhaan Ahmad**[a,c,*]

[a] Cardiovascular Institute, University of Pittsburgh, Pittsburgh, PA 15213

[b] Renal-Electrolyte Division, Department of Medicine, University of Pittsburgh, Pittsburgh, PA 15213

[c] Department of Human Genetics, University of Pittsburgh, Pittsburgh, PA 15213

Abstract

Human mutations in the gene *PRKAG2* encoding the γ2 subunit of AMP-activated protein kinase (AMPK) cause a glycogen storage cardiomyopathy. Transgenic mice (TG^{T400N}) with the human T400N mutation exhibit inappropriate activation of AMPK and consequent glycogen storage in the heart. Although increased glucose uptake and activation of glycogen synthesis have been documented in *PRKAG2* cardiomyopathy, the mechanism of increased glucose uptake has been uncertain. Wildtype (WT), TG^{T400N}, and $TG^{\alpha 2DN}$ (carrying a dominant negative, kinase dead α2 catalytic subunit of AMPK) mice were studied at ages 2–8 weeks. Cardiac mRNA expression of sodium-dependent glucose transporter 1 (SGLT1), but not facilitated-diffusion glucose transporter 1 (GLUT1) or GLUT4, was increased ~5–7 fold in TG^{T400N} mice relative to WT. SGLT1 protein was similarly increased at the cardiac myocyte sarcolemma in TG^{T400N} mice. Phlorizin, a specific SGLT1 inhibitor, attenuated cardiac glucose uptake in TG^{T400N} mice by ~40%, but not in WT mice. Chronic phlorizin treatment reduced cardiac glycogen content by ~25% in TG^{T400N} mice. AICAR, an AMPK activator, increased cardiac SGLT1 mRNA expression ~3 fold in WT mice. Relative to TG^{T400N} mice, double transgenic ($TG^{T400N}/TG^{\alpha 2DN}$) mice had decreased (~50%) cardiac glucose uptake and decreased (~70%) cardiac SGLT1 expression. TG^{T400N} hearts had increased binding activity of the transcription factors HNF-1 and Sp1 to the promoter of the gene encoding SGLT1. Our data suggest that upregulation of cardiac SGLT1 is responsible for increased cardiac glucose uptake in the TG^{T400N} mouse. Increased AMPK activity leads to upregulation of SGLT1, which in turn mediates increased cardiac glucose uptake.

Keywords

cardiomyopathy; energy; functional genomics; genetics; genetically altered mice; glucose; membrane transport; metabolism; molecular biology

[*]Corresponding author: Ferhaan Ahmad, MD, PhD, Cardiovascular Institute, University of Pittsburgh, 200 Lothrop Street, Suite S-558, Mail Stop HPU 01 05 05, Pittsburgh, PA 15213-2582; Telephone: 412-648-9286; Facsimile: 412-648-5991; ahmadf@upmc.edu.

Disclosures

None.

1. Introduction

The 5'AMP-activated protein kinase (AMPK) is a widely expressed enzyme which serves as a cellular energy gauge, maintaining fuel supply by activating and inhibiting energy-generating and energy-consuming pathways, respectively. Mutations in the gene *PRKAG2*, encoding the γ2 subunit of AMPK, have been demonstrated to produce a distinct cardiomyopathy in human families characterized by glycogen storage, ventricular hypertrophy, ventricular preexcitation, and progressive conduction system disease [1–3]. The association between *PRKAG2* mutations and glycogen storage cardiomyopathy has been confirmed in four different transgenic mouse models [4–7]. Inappropriate activation of AMPK appears to be the primary consequence of at least some *PRKAG2* mutations, although inactivation of AMPK has been suggested in other mutations [2,7–9]. We have shown in two transgenic models with the T400N and N488I mutations, respectively, that the disease phenotype can be attenuated by genetically reducing AMPK activity, suggesting that the functional effect of these mutations is a gain of function of the catalytic activity [3,7].

In transgenic mice with the N488I mutation, Luptak and colleagues demonstrated increases in cardiac glucose uptake and glycogen synthesis [10]. However, the mechanism of increased cardiac glucose uptake remained uncertain. There are two families of cellular glucose transporters: the facilitated-diffusion glucose transporter (GLUT) family; and the sodium-dependent glucose transporter (SGLT) family [11]. SGLTs transport glucose by a secondary active transport mechanism which uses the sodium concentration gradient established by the Na^+/K^+-ATPase pump. Classically, it has been thought that only the GLUT isoforms GLUT1 and GLUT4 are responsible for glucose uptake in cardiac myocytes [12]. However, we have recently reported that the SGLT isoform SGLT1 is present at the protein level in cardiac myocytes, and appears to be localized to the sarcolemma [13]. In this study, we show that SGLT1 is upregulated in transgenic mice with the T400N mutation (TG^{T400N}); that SGLT1 at least partially mediates increased cardiac glucose uptake in TG^{T400N} mice; that the disease phenotype is partially attenuated by inhibition of SGLT1; and that the upregulation of cardiac SGLT1 is caused by AMPK activity.

2. Materials and methods

2.1. Mice

Transgenic mice (TG^{T400N}) with cardiac myocyte-specific overexpression of human *PRKAG2* cDNA with the T400N mutation in the FVB background have been previously described [7,14]. These mice recapitulate the human glycogen storage cardiomyopathy phenotype. $TG^{\alpha 2DN}$ mice, which overexpress a dominant negative, kinase dead mutant of the AMPK α2 catalytic subunit and have low cardiac myocyte AMPK activity, were a generous gift of Rong Tian, MD, PhD [15]. Double transgenic mice ($TG^{T400N}/TG^{\alpha 2DN}$) were obtained by crossbreeding. Wildtype (WT) littermates were used as controls. In general, experiments requiring harvests of cardiac tissue were performed at the same time of the day, approximately 10 AM, after 2 h of fasting.

All experiments using mice were consistent with the *Guide for the Care and Use of Laboratory Animals* (US National Institutes of Health Publication No. 85–23, revised 1996) and were approved by the University of Pittsburgh Institutional Animal Care and Use Committee.

2.2. Osmotic minipumps for chronic phlorizin delivery to mice

Osmotic minipumps (Alzet) were filled to deliver phlorizin (Sigma), a specific SGLT1 inhibitor, to mice chronically at a dose of 100 mg/kg/day. Phlorizin was dissolved in a solution containing 10% ethanol, 15% DMSO, and 75% saline. In control mice, minipumps were filled

with identical vehicle without phlorizin. Minipumps were implanted in the interscapular area of 2 week old male mice after sedation with tribromoethanol (125 mg/kg IP) as previously described [16].

2.3. In vivo cardiac glucose uptake

Basal cardiac glucose uptake was measured in mice as described [13]. In brief, mice were administered 2-deoxy-D-[1-^{14}C]-glucose (2-[^{14}C]DG) (10 μCi) intraperitoneally. After 30 min, mice were sacrificed and their hearts rapidly excised. Hearts were homogenized in 10 volumes of phosphate-buffered saline (PBS), and radioactivity in 20 μl of homogenate was measured in a liquid scintillation counter. Because 2-deoxy-D-glucose is phosphorylated but not further metabolized, it remains trapped inside cells. Thus, glucose uptake was estimated by determining cardiac radioactivity. These cardiac glucose uptake assays were performed in the following male mice at age 6–8 weeks: WT and TG^{T400N} mice 10 min following the administration of phlorizin (400 mg/kg intraperitoneally [IP]), indinavir (10 mg/kg IP), or vehicle; and TG^{T400N}/TG$^{\alpha 2DN}$ mice. Phlorizin (Sigma), a specific SGLT1 inhibitor, was dissolved at a concentration of 30 mg/ml in 10% ethanol, 15% DMSO, and 75% saline. Indinavir (Fisher), a GLUT inhibitor, was dissolved in water at a concentration of 2.5 mg/ml.

2.4. RNA isolation and real-time quantitative PCR (QPCR)

Total RNA was isolated from whole heart with TRIzol (Invitrogen). Reverse transcriptase reactions were performed as described [17] using the Superscript III First-Strand Kit (Invitrogen) for first-strand cDNA synthesis. Primers for real-time quantitative PCR (QPCR) analysis were designed using published sequence information, avoiding regions of homology with other genes (Table). Ten ng of cDNA were analyzed on an ABI PRISM 7700 using Absolute SYBR Green ROX PCR Master Mix (Thermo Scientific). Fold-changes were calculated after normalization to cyclophilin transcript levels.

2.5. Protein extraction and membrane protein fractionation

Extraction of total cardiac protein was performed as described previously [14]. The preparation and fractionation of membranes from cardiac tissue was performed using a commercially available plasma membrane protein extraction kit (BioVision, #k268-50) according to the manufacturer's instructions. For membrane fractionation, 10–12 pooled hearts of each genotype at ages 2 and 8 weeks, totaling at least 1 g in mass, were homogenized and processed for extraction of total membrane protein (comprising sarcolemmal and intracellular membrane bound proteins) or sarcolemmal membrane protein. The protein content in each fraction was measured by Bradford reagent (Bio-Rad). The α1 subunit of the Na^+/K^+-ATPase, a sarcolemmal membrane marker, was measured by immunoblot to document adequate enrichment of membrane fractions.

2.6. Analysis of protein expression

Immunoblotting, autoradiography, and densitometry were performed as described previously [14]. An equal amount (50–100 μg) of protein was separated by sodium dodecylsulfate polyacrylamide gel electrophoresis (SDS-PAGE). For membrane fractionation studies, each lane was loaded with extracts from 10–12 pooled hearts of each genotype at ages 2 and 8 weeks; for all other studies, each lane was loaded with protein extracts from individual hearts as indicated in the figures. After electrophoresis, proteins were transferred to PVDF membranes (Amersham Biosciences). The membranes were then blocked in Tris-buffered saline Tween-20 (TBS-T; 10 mM Tris, pH 7.5, 150 mM NaCl, 0.05% Tween-20) and 5% non-fat dry milk for 1 h, and subsequently washed and incubated with primary antibodies in TBS-T and 2% bovine serum albumin (BSA) at 4 °C overnight. The following antibodies and titers were used: AMPKα (1:1000 dilution, Cell Signaling, # 2532), phospho-Thr^{172} AMPKα (1:1000 dilution,

Cell Signaling, # 2531), GLUT1 (1:5000 dilution, Abcam, # ab40084), GLUT4 (1:1000 dilution, Cell Signaling, #2299), Na^+/K^+-ATPase α1 (1:1000 dilution, Cell Signaling, #3010), and SGLT1 (1:200 dilution, Santa Cruz, # sc-20582). After washing with TBS-T, membranes were incubated with anti-rabbit (1:10000 dilution, Amersham, #NA934V) or anti-goat (1:2000 dilution, Santa Cruz, sc-2020) horseradish peroxidase conjugated secondary antibody for 1 h. Signal was detected by chemiluminescence using the ECL detection system (Amersham). Gel staining with Coomassie Blue was used as an internal control for equal loading of protein. Quantification of bands on X-ray film was performed using Image J Software (NIH).

2.7. Tissue fixation and immunofluorescence staining

Mouse cardiac tissue was processed for immunofluorescence of SGLT1 as described previously [18]. Hearts were fixed for 4 h at room temperature in PBS containing 4% paraformaldehyde, 10 mM sodium periodate, 70 mM lysine, and 5% sucrose (PLP), washed in PBS, and quenched in NH_4Cl [19]. Tissues were cryoprotected in a solution of 30% sucrose in PBS overnight at 4°C. These tissues were embedded in OT compound (Tissue TEK, Sakura Finetek) and mounted on a cutting block. After being frozen in a Reichert Frigocut microtome, sections were picked up on Superfrost Plus slides (Fisher). Immunofluorescence staining was performed on 4-μm cryostat sections after SDS antigen retrieval [20]. Slides were washed in PBS followed by incubation with a blocking solution containing 1% bovine serum albumin in PBS-0.02% sodium azide for 15 min. Tissues were labeled using anti-murine SGLT1 antibody (1:200 in DAKO diluent, raised in goat, Santa Cruz, #sc20582) for 75 min sections followed by labeling with a secondary antibody (DAG-FITC 1:100, Jackson Immunologicals). For co-immunolocalization studies, tissues were incubated with anti-murine SGLT1 antibody (1:75 dilution) and an antibody against the Na^+/K^+-ATPase (1:25 dilution, raised in rabbit, Cell Signaling, #3010) overnight on the same tissues. After each antibody incubation, sections were washed twice for 5 min in high-salt PBS (2.7% NaCl) and once in PBS, and then incubated for 1 h with secondary antibodies, donkey anti-rabbit FITC and donkey anti-goat-CY3 (1:100 and 1:800 dilution, respectively, both from Jackson Immunologicals). After repeating the same series of washes as above, the slides were mounted with Vectashield (Vector Labs). Parallel control incubations omitting the primary antibody ("no-primary" control, using DAKO reagent alone) or using a nonspecific primary antibody were performed. For the nonspecific primary antibody control, IgG goat (1ug/ul, 1:375 dilution in DAKO diluent, Sigma #I5256) was used on tissue from an 8 week old WT mouse for 75 min (0.002666667 ug/ul) followed by DAG-CY3. The SGLT1 immunizing peptide used to produce this antibody was employed for peptide inhibition controls as previously reported [13,21]. Images were obtained using a Leica Confocal microscope. The acquisition settings for the immunolabeled tissues and the no-primary controls were identical.

2.8. Cardiac glycogen content

Cardiac glycogen content was determined by the amyloglucosidase digestion method as we have previously reported [7].

2.9. Chromatin Immunoprecipitation (ChIP)

Chromatin immunoprecipitation (ChIP) assays for binding activity of specificity protein 1 (Sp1) and hepatocyte nuclear factor 1 (HNF-1) to the promoter of the gene encoding SGLT1 were performed as described [22]. For each individual assay, approximately 30 mg of starting cardiac tissue was used to harvest chromatin, and 0.45 μg of antibody was added to each sample. The following antibodies were used: HNF-1 (Santa Cruz, # sc-8986) and Sp-1 (Santa Cruz, sc-17824). QPCR primers used to quantify protein-DNA interaction are listed in the Table. For Sp1, the primers were designed to quantify total binding activity at both Sp1 sites.

2.10. Statistical analysis

Results are expressed as mean ± SE. Differences between two groups were compared by Student's *t* test, and among multiple groups by one-way ANOVA with post hoc Bonferroni test. A *p*-value of less than 0.05 was considered significant.

3. Results

3.1. TG^{T400N} hearts exhibit increased glucose uptake

We previously reported the presence of increased cardiac glycogen in TG^{T400N} mice up to age 8 weeks [7]. Therefore, in the current study we measured *in vivo* cardiac glucose uptake in TG^{T400N} mice and WT littermates at ages 2 and 8 weeks. Significant increases in cardiac glucose uptake were observed at ages 2 weeks (~1.5 fold) and 8 weeks (~2.5 fold) in TG^{T400N} mice relative to WT (Fig. 1). These findings corroborate those reported by Luptak and colleagues in transgenic mice with the N488I mutation [10].

3.2. TG^{T400N} hearts exhibit increased expression of genes in the glycogen synthetic pathway

We quantified cardiac mRNA expression of three genes involved in the glycogen synthesis pathway in TG^{T400N} mice and WT littermates at ages 2 and 8 weeks: UDP glucose pyrophosphorylase 2 (UDPG-PPL2), glycogen synthase 1 (GYS1), and glucan branching 1 (GBE1). GYS1 and GBE1 expression were significantly increased 3–10 fold in TG^{T400N} hearts relative to WT at both ages 2 and 8 weeks; UDPG-PPL2 expression was increased 2.5-fold in TG^{T400N} hearts only at age 8 weeks (Fig. 2). The upregulation of expression of these genes is consistent with an increase in glycogen synthesis in TG^{T400N} hearts, ultimately leading to excess cardiac glycogen. These findings are similar to those reported in transgenic mice with the N488I mutation [10].

3.3. GLUT1, but not GLUT4, expression is increased in TG^{T400N} hearts

Classically, it has been thought that only GLUT1 and GLUT4 are responsible for glucose uptake in cardiac myocytes [12]. Consistent with this paradigm, increased cardiac expression of GLUT1 and GLUT4 has been found in different animal models that have increased cardiac glucose uptake [23–25]. Therefore, we quantified GLUT1 and GLUT4 in TG^{T400N} hearts at the levels of total cellular mRNA, total cellular protein, total membrane protein (comprising sarcolemmal and intracellular membrane bound proteins), and sarcolemmal protein fraction. There were no significant changes in cardiac GLUT1 and GLUT4 transcript levels as assessed by QPCR in TG^{T400N} mice relative to WT littermates at ages 2 and 8 weeks (Fig. 3A). However, GLUT1 protein expression was significantly increased (>1.6 fold) in extracts of total cellular protein from TG^{T400N} mice relative to WT littermates at ages 2 and 8 weeks (Fig. 3B). Although GLUT1 protein expression was not significantly increased in extracts of total membrane protein from TG^{T400N} mice relative to WT littermates at ages 2 and 8 weeks (Fig. 3C), GLUT1 protein expression was increased in extracts of sarcolemmal membrane protein from TG^{T400N} mice relative to WT littermates at age 8 weeks (Fig. 3D).

In contrast, GLUT4 protein expression was either unchanged or decreased in TG^{T400N} mice relative to WT littermates. Specifically, GLUT4 protein expression was significantly decreased in extracts of total cellular protein from TG^{T400N} mice relative to WT littermates at ages 2 and 8 weeks (Fig. 3B). GLUT4 protein expression was not significantly different in extracts of total membrane protein from TG^{T400N} mice relative to WT littermates at ages 2 and 8 weeks (Fig. 3C). AMPK activation is associated with translocation of GLUT4 to the sarcolemma, promoting glucose uptake [26,27]. Because we have previously shown inappropriate activation of AMPK in TG^{T400N} hearts [7], we measured GLUT4 in extracts of sarcolemmal membrane

protein. However, there were no differences found in sarcolemmal GLUT4 protein expression between TG^{T400N} mice and WT littermates (Fig. 3D).

3.4. Increased glucose uptake in TG^{T400N} hearts is associated with increased expression of SGLT1

We have previously reported that SGLT1 protein is present in cardiac myocytes and appears to be localized to the sarcolemma, and that its expression is perturbed in several disease states [13]. Therefore, we next quantified SGLT1 in TG^{T400N} hearts at the levels of total cellular mRNA, total cellular protein, total membrane protein, and sarcolemmal protein fraction. Cardiac SGLT1 transcript levels as assessed by QPCR were significantly upregulated ~7 fold and ~5 fold, respectively, in TG^{T400N} mice relative to WT littermates at ages 2 and 8 weeks (Fig. 3A). However, SGLT1 protein expression was not elevated in extracts of total cellular protein from TG^{T400N} mice relative to WT littermates at ages 2 and 8 weeks (Fig. 3B). Despite a lack of increase in total cellular SGLT1 protein, an increase in membrane bound SGLT1 protein was evident. Similar increases in SGLT1 protein expression were observed in extracts of total membrane protein from TG^{T400N} mice relative to WT littermates at ages 2 and 8 weeks (Fig. 3C), and in extracts of sarcolemmal membrane protein from TG^{T400N} mice relative to WT littermates (Fig. 3D).

Immunofluorescence studies corroborated our membrane fractionation studies. SGLT1 had similar subcellular distributions in cardiac myocytes from TG^{T400N} mice relative to WT littermates at ages 2 and 8 weeks incubated under the same conditions and using identical laser and acquisition settings (Fig. 3E). Furthermore, there was partial co-localization of SGLT1 and Na^+/K^+-ATPase, a sarcolemmal membrane marker, in cardiac myocytes from 8 week old WT and TG^{T400N} mice (Fig. 3F, left vs. right).

3.5. SGLT1 inhibition attenuates cardiac glucose uptake and glycogen deposition in TG^{T400N} hearts to a greater degree than does GLUT inhibition

To determine whether the increased SGLT1 expression in TG^{T400N} hearts was partially or completely responsible for the increased cardiac glucose uptake that we had observed, we measured cardiac glucose uptake in 4–6 week old TG^{T400N} mice in the presence of phlorizin, a specific inhibitor of SGLT1. Whereas acute administration of phlorizin (400 mg/kg IP) had no effect on cardiac glucose uptake in WT mice (Fig. 4A), it significantly reduced cardiac glucose uptake in TG^{T400N} mice (Fig. 4B).

Since increased cardiac glucose uptake is thought to lead to increased cardiac glycogen deposition in *PRKAG2* cardiomyopathy [10], we hypothesized that chronic inhibition of SGLT1 would attenuate this glycogen deposition. Subcutaneous osmotic minipumps delivering phlorizin (100 mg/kg/day) or inert vehicle were implanted in 2 week old TG^{T400N} mice. Four weeks later, mice were sacrificed for harvest of hearts. A ~25% reduction in cardiac glycogen content was observed in TG^{T400N} mice treated chronically with phlorizin relative to TG^{T400N} mice administered inert vehicle (Fig. 4C).

In addition to SGLT1, GLUT1 was upregulated in TG^{T400N} mice. Furthermore, even though GLUT4 expression was not increased and localization was unperturbed in TG^{T400N} hearts, increases in its affinity or activity may still contribute to increased cardiac glucose uptake. To determine the relative contributions of GLUT1 and GLUT4 to increased cardiac glucose uptake, we administered indinavir (10 mg/kg IP), a GLUT inhibitor, to TG^{T400N} mice and WT littermates, and measured cardiac glucose uptake. Although WT mice exhibited a significant reduction in cardiac glucose uptake (Fig. 5A), no significant reduction was observed in TG^{T400N} mice (Fig. 5B). Combined with our observations with phlorizin, these data suggest

that SGLT1 may be a greater contributor than GLUT1 and GLUT4 to the increased cardiac glucose uptake in TG^{T400N} mice.

3.6. AMPK regulates cardiac SGLT1 expression

We have previously shown that TG^{T400N} mice initially have inappropriate activation of AMPK [7]. To determine whether AMPK activation may be associated with increased cardiac SGLT1 expression, 8 week old WT mice were administered aminoimidazole carboxamide ribonucleotide (AICAR), a pharmacological activator of AMPK, at a dose of 500 μg/kg IP twice at 3 h intervals. Mice were sacrificed 3 h following the second AICAR dose, and hearts harvested. Phosphorylation of the α subunit of AMPK, which correlates with AMPK activity [7], was increased (Fig. 6A). AMPK activation in mice receiving AICAR was associated with increased cardiac SGLT1 mRNA expression (Fig. 6B).

$TG^{\alpha 2DN}$ mice, which overexpress a dominant negative mutant of the AMPK α2 catalytic subunit and have low cardiac myocyte AMPK activity, have been previously described [15]. Double transgenic mice ($TG^{T400N}/TG^{\alpha 2DN}$) were obtained by crossbreeding. $TG^{T400N}/TG^{\alpha 2DN}$ mice showed attenuation of AMPK overactivity (Fig. 6C), and we have previously shown that these mice exhibit an attenuation of the phenotype relative to TG^{T400N} [7]. $TG^{T400N}/TG^{\alpha 2DN}$ mice had attenuated cardiac glucose uptake (Fig. 6D) concurrent with a decrease in SGLT1 transcript and protein expression (Figs. 6E to 6G). Therefore, cardiac AMPK activity, SGLT1 expression, and glucose uptake appear to be associated.

The promoter of the *SLC5A1* gene encoding SGLT1 contains three cis elements that increase transcription—one binding site for hepatocyte nuclear factor 1 (HNF-1) and two binding sites for specificity protein 1 (Sp1) [28]. Therefore, we performed chromatin immunoprecipitation (ChIP) assays in TG^{T400N} and WT hearts to measure binding activity of these transcription factors to the promoter. For Sp1, total binding activity at both Sp1 sites together was quantified. Increased expression of SGLT1 in TG^{T400N} hearts was associated with increased binding activity of both HNF-1 and Sp1 (Figs. 6H and 6I).

4. Discussion

In this study, we have determined that SGLT1 is upregulated in a transgenic mouse with the T400N mutation in *PRKAG2* previously identified in human subjects with glycogen storage cardiomyopathy; that SGLT1 appears to mediate at least part of the increased cardiac glucose uptake and glycogen deposition in this mouse; that inhibition of SGLT1 attenuates the disease phenotype; and that AMPK appears to regulate SGLT1 expression in the heart.

Human mutations in *PRKAG2* lead to excess glycogen storage in several transgenic mouse models [4–7]. Although increased cardiac glucose uptake and activation of glycogen synthesis enzymes was documented in a transgenic mouse expressing the N488I mutation [10], the glucose transporter responsible for increased cardiac glucose uptake was not defined. Similarly, in transgenic mice with an R225Q mutation in the γ3 subunit of AMPK, skeletal muscle showed increased expression of glycogen synthesis genes [29]. UDPG-PPL was also upregulated in the skeletal muscle of carriers of the porcine RN- mutation in the γ3 subunit of AMPK [30]. Consistent with these studies, we observed increased cardiac glucose uptake and increased cardiac expression of genes in the glycogen synthesis pathway, including UDPG-PPL2, GYS1, and GBE1, in TG^{T400N} mice.

Other animal models with increased cardiac glucose uptake exhibit increased expression of GLUT1 and GLUT4 [23–25]. Since activation of AMPK promotes translocation of GLUT4 to the sarcolemma in cardiac myocytes [31], and we have documented early inappropriate activation of AMPK in the TG^{T400N} heart [7], we analyzed cardiac GLUT1 and GLUT4

expression and localization in this model. GLUT1 protein expression was increased and GLUT4 protein was unchanged or decreased in extracts of total cellular protein and sarcolemmal membrane protein at ages 2 and 8 weeks. Moreover, administration of indinavir, a GLUT inhibitor, to TG^{T400N} mice did not significantly inhibit cardiac glucose uptake. These findings suggest that, although GLUT1 expression is increased, GLUT1 and GLUT4 may not be the most important contributors to the pathogenesis of the cardiomyopathy in TG^{T400N} mice.

Although the facilitated-diffusion glucose transporters GLUT1 and GLUT4 have classically been thought to be responsible for glucose uptake in cardiac myocytes [12], a previous study showed that the expression of the sodium-dependent glucose transporter SGLT1 mRNA in the human heart was unexpectedly about 10-fold higher than in the kidney [32]. We have recently determined that SGLT1 is present at the protein level in cardiac myocytes, and appears to be localized to the sarcolemma [13]. We have now confirmed that SGLT1 partially co-localizes with the Na^+/K^+-ATPase, a sarcolemmal membrane marker, in cardiac myocytes (Fig. 3F). The expression and function of SGLT1 has been previously established in small intestinal enterocytes and renal proximal tubule S3 cells, where it mediates glucose uptake using the sodium concentration gradient established by Na^+/K^+ ATPase pump [11]. SGLT1 has a mass of 73 kDa, 664 amino acids, and 14 membrane spans [33]. The transport cycle begins with two external Na^+ ions binding to the SGLT1 and causing a conformational change that results in an increase in affinity for glucose. Glucose binding induces a second conformational change to expose the ligand-binding sites to the internal membrane surface, where glucose is released into the cytoplasm, followed by the Na^+ ions. SGLT1 then returns to its initial conformation [34]. The gene encoding SGLT1 is solute carrier family 5 member 1 (*SLC5A1*) [35,36]. The *SLC5A1* promoter contains three cis elements which increase transcription—one binding site for hepatocyte nuclear factor 1 (HNF-1) and two binding sites for specificity protein 1 (Sp1) [28,37]. Sp1 is known to mediate gene expression changes in response to insulin and glucagon [38]. Moreover, SGLT1 can be phosphorylated by protein kinases A (PKA) and C (PKC) at Tyr^{50}, Ser^{303}, Ser^{418}, and Tyr^{635} [33], which causes translocation of SGLT1 from intracellular vesicles to the plasma membrane and an increase in glucose uptake [39,40]. In enterocytes, intracellular SGLT1 is sequestered in compartments associated with microtubules that are a reserve pool that can be recruited to the cell surface by exocytosis [41,42].

Having determined that SGLT1 protein is present in cardiac myocytes and is localized to the sarcolemma, we examined whether SGLT1 is responsible for the increased glucose uptake in TG^{T400N} hearts. We observed a ~5–7-fold increase in SGLT1 transcript in the hearts of TG^{T400N} mice at ages 2 and 8 weeks. Although total cellular SGLT1 protein was not increased in TG^{T400N} mice at ages 2 and 8 weeks, total cellular membrane and sarcolemmal protein extracts from TG^{T400N} hearts exhibited increased levels of SGLT1. These data suggest that SGLT1 is upregulated to the sarcolemma in TG^{T400N} hearts. To determine whether this upregulation of SGLT1 was associated with increased cardiac glucose uptake, we inhibited SGLT1 activity using phlorizin both acutely (3 hours) and chronically (4 weeks). Increased cardiac glucose uptake in TG^{T400N} mouse was significantly inhibited by acute phlorizin administration. Furthermore, chronic phlorizin administration resulted in a reduction in cardiac glycogen content in TG^{T400N} mice. Therefore, SGLT1 appears chronically to mediate increased glucose uptake in *PRKAG2* cardiomyopathy. Moreover, the differential effect of GLUT and SGLT1 inhibitors on cardiac glucose uptake in TG^{T400N} and WT mice suggests that cardiac SGLT1 has a particularly important role in pathological or stressed states, relative to baseline conditions.

It should be noted that mRNA and protein measurements for GLUT1, GLUT4, and SGLT1 were not fully concordant. For example, although GLUT1 mRNA was unchanged in TG^{T400N} mice relative to WT littermates, GLUT1 protein was increased. In contrast, SGLT1 mRNA was increased at the total cell level, SGLT1 protein was unchanged at the total cell

level, and SGLT1 protein was increased at the total membrane and sarcolemmal membrane levels. We speculate that these findings may be related to differences in post-transcriptional events, including protein stability and localization, ultimately leading to differences in activity and impact on cardiac glucose uptake.

The attenuation of glucose uptake and cardiac glycogen content following acute and chronic phlorizin administration, respectively, in TG ^{T400N} mice points to SGLT1 as a potential target for treatment in *PRKAG2* cardiomyopathy and possibly other glycogen storage cardiomyopathies. Phlorizin is an organic compound consisting of a glucose moiety and two aromatic rings joined by an alkyl spacer [43]. It is a competitive inhibitor that appears to interact with SGLT1 at two distinct sites [44]. The glucose moiety binds to the substrate binding site, and the aromatic rings bind to a second site located in a large loop between transmembrane helices 13 and 14. Although phlorizin is not in routine clinical use, it has been used experimentally in diabetes to lower plasma glucose concentrations independent of insulin. Its ability to inhibit intestinal glucose absorption and renal glucose resorption suggests a potential role in treating obesity. It may even have a role in the treatment of malaria, since it has been shown to inhibit pores that are induced by the parasite in the host erythrocyte cell membrane and that are necessary for parasite growth [45]. However, because phlorizin is metabolized and poorly absorbed in the intestine, parenteral administration would be necessary in the treatment of cardiac disease. Newer compounds such as T-1095 and sergliflozin currently in development may not be subject to this drawback.

Since TG^{T400N} hearts exhibit early activation of AMPK [7], we hypothesized that AMPK upregulates SGLT1 in cardiac myocytes. Administration of AICAR, an AMPK activator, to WT mice significantly increased cardiac SGLT1 protein expression. Moreover, when AMPK was genetically inhibited by crossing TG^{T400N} with TG$^{\alpha 2DN}$ mice, double transgenic mice (TG^{T400N}/TG$^{\alpha 2DN}$) exhibited lower AMPK activity, decreased cardiac SGLT1 expression, and decreased cardiac glucose uptake. These findings are consistent with both a role for AMPK in the regulation of SGLT1 in cardiac myocytes, and a central role for SGLT1 in the pathogenesis of *PRKAG2* cardiomyopathy. Furthermore, AMPK α2 catalytic subunit activity appears to be responsible for upregulation of SGLT1 through chronic transcriptional effects.

Additional evidence implicates AMPK in upregulation of SGLT1 in cardiac myocytes. We previously reported that acute administration of the hormone leptin leads to upregulation of cardiac SGLT1 transcript and an increase in cardiac glucose uptake, which can be inhibited by the SGLT1 inhibitor phlorizin [13]. Leptin has been shown to activate AMPK in skeletal muscle [46]. We have also shown that cardiac ischemia, which activates AMPK [26], leads to upregulation of SGLT1 expression [13]. AMP, which activates AMPK, has been shown to increase SGLT1 expression rapidly in the small intestine [47]. In *Xenopus* oocytes coexpressing SGLT1 and constitutively active α^{R70Q}AMPK (α1β1γ1(R70Q)), AMPK activation enhanced maximal currents but not substrate affinity of the transporter [48], consistent with an effect on plasma membrane expression. Furthermore, the AMPK activators AICAR, phenformin, and A-769662 increased SGLT1 protein abundance in the plasma membrane of Caco2 cells. However, there is also conflicting evidence in the literature that suggests the relationship between AMPK and SGLT1 is likely complex. AICAR has been reported to decrease SGLT1 expression in the jejunum [49]. Thus, there may be differences between acute and chronic AMPK regulation of SGLT1, and differences among tissues, cell types, and possibly species.

The precise mechanism by which AMPK upregulates SGLT1 in cardiac myocytes remains to be fully elucidated. Our data suggest that AMPK exerts a chronic transcriptional effect on SGLT1. The promoter of the gene *SLC5A1* encoding SGLT1 contains three cis elements that increase transcription—one binding site for hepatocyte nuclear factor 1 (HNF-1) and two

binding sites for specificity protein 1 (Sp1) [28]. Our ChIP assays have shown increased binding activity of both HNF-1 and Sp1 to the *SLC5A1* promoter. Although at present AMPK is not known to target Sp1 or HNF-1, Sp1 binding activity in general is known to be increased by phosphorylation by other kinases [50]. Therefore, it is likely that AMPK stimulates SGLT1 transcription via these transcription factors, although it may also act on one of the putative binding sites for other transcription factors found on the promoter. In other tissues, phosphorylation of SGLT1 causes translocation of SGLT1 from intracellular vesicles to the plasma membrane and an increase in glucose uptake [39]. AMPK may directly or indirectly mediate SGLT1 phosphorylation. AMPK indirectly increases phosphatidylinositol 3-kinase (PI-3K) activity [51], and PI-3K activity in turn has been shown to regulate translocation of SGLT1 [52]. Another mechanism is suggested by the observations that the protein HuR increases SGLT1 mRNA stability by binding to a critical uridine-rich element (URE) in its 3' untranslated region [53], and in hepatocytes AMPK stimulates the binding of HuR to its targets [54]. Based on our data and evidence from the literature as outlined above, Fig. 7 presents a hypothetical model of the mechanism by which increased AMPK activity leads to increased cardiac glucose uptake via SGLT1 in *PRKAG2* cardiomyopathy. Further studies will be required to validate this model fully.

A potential limitation of this study is that cardiac glycogen levels, metabolic regulation, and substrate utilization show substantial diurnal variations. Furthermore, expression of SGLT1 in the gastrointestinal tract exhibits diurnal rhythmicity in concert with clock genes that is independent of local luminal nutrient delivery [55,56]. Therefore, the results of our experiments, performed at one standard time of the day, may not be fully generalizable to other times of the day.

Another potential limitation of this study is that only male mice were studied in detail. Sex influences phenotype severity in other cardiomyopathies [57]. However, differences in disease phenotype based on sex have not been clearly documented in *PRKAG2* cardiomyopathies, and our own preliminary unpublished data in both human subjects and murine models suggest that our findings in this study are applicable to both sexes.

In conclusion, our data suggest that inappropriate activation of AMPK, secondary to the T400N mutation in *PRKAG2*, leads to increased cardiac SGLT1 expression, which in turn is responsible for increased cardiac glucose uptake. While this study shows for the first time a functional role of SGLT1 in cardiac disease, our previously reported work suggests that this transporter is relevant far beyond *PRKAG2* cardiomyopathy and is a heretofore unrecognized participant in adaptive or maladaptive responses of the heart to a wide range of pathological insults. SGLT1 expression is perturbed in diabetic cardiomyopathy and ischemic heart disease, and functional improvement in failing left ventricles is associated with upregulation of SGLT1 [13]. As discussed above, AMPK and leptin, both of which mediate cardiac response to ischemia, may exert their effects in part through SGLT1. Thus, SGLT1 may represent an entirely novel therapeutic target in the heart, and agents that directly modify cardiac SGLT1 expression, localization, and activity may be useful in the modulation of cardiac energy substrate utilization and in the treatment of glycogen storage cardiomyopathy, ischemic heart disease, and other cardiac diseases.

Acknowledgments

This work was supported by an American Heart Association Scientist Development Grant 053531N (FA); Postdoctoral Fellowships from the American Heart Association and the Hillgrove Foundation (SKB); NIH/NIDDK grants P30 DK-079307 "Pittsburgh Kidney Research Center" and R01 DK075048 (KRH); an American Heart Association Grant-in-Aid 09GRNT2060539 (NMPS); an NIH/NIDDK grant R01 DK084184 (NMPS); and the Cardiovascular Institute of the University of Pittsburgh (Barry London, Director) (FA). FA is a Doris Duke Charitable Foundation Clinical Scientist. We acknowledge Christy Smolak for excellent technical support.

References

1. Gollob MH, Green MS, Tang AS, Gollob T, Karibe A, Ali Hassan AS, et al. Identification of a gene responsible for familial Wolff-Parkinson-White syndrome. N Engl J Med 2001;344:1823–31. [PubMed: 11407343]
2. Arad M, Benson DW, Perez-Atayde AR, McKenna WJ, Sparks EA, Kanter RJ, et al. Constitutively active AMP kinase mutations cause glycogen storage disease mimicking hypertrophic cardiomyopathy. The Journal of clinical investigation 2002;109:357–62. [PubMed: 11827995]
3. Ahmad F, Arad M, Musi N, He H, Wolf C, Branco D, et al. Increased alpha2 subunit-associated AMPK activity and PRKAG2 cardiomyopathy. Circulation 2005;112:3140–8. [PubMed: 16275868]
4. Arad M, Moskowitz IP, Patel VV, Ahmad F, Perez-Atayde AR, Sawyer DB, et al. Transgenic mice overexpressing mutant PRKAG2 define the cause of Wolff-Parkinson-White syndrome in glycogen storage cardiomyopathy. Circulation 2003;107:2850–6. [PubMed: 12782567]
5. Sidhu JS, Rajawat YS, Rami TG, Gollob MH, Wang Z, Yuan R, et al. Transgenic mouse model of ventricular preexcitation and atrioventricular reentrant tachycardia induced by an AMP-activated protein kinase loss-of-function mutation responsible for Wolff-Parkinson-White syndrome. Circulation 2005;111:21–9. [PubMed: 15611370]
6. Davies JK, Wells DJ, Liu K, Whitrow HR, Daniel TD, Grignani R, et al. Characterization of the role of gamma2 R531G mutation in AMP-activated protein kinase in cardiac hypertrophy and Wolff-Parkinson-White syndrome. Am J Physiol Heart Circ Physiol 2006;290:H1942–51. [PubMed: 16339829]
7. Banerjee SK, Ramani R, Saba S, Rager J, Tian R, Mathier MA, et al. A PRKAG2 mutation causes biphasic changes in myocardial AMPK activity and does not protect against ischemia. Biochem Biophys Res Commun 2007;360:381–7. [PubMed: 17597581]
8. Hamilton SR, Stapleton D, O'Donnell JB Jr, Kung JT, Dalal SR, Kemp BE, et al. An activating mutation in the gamma1 subunit of the AMP-activated protein kinase. FEBS Lett 2001;500:163–8. [PubMed: 11445078]
9. Daniel T, Carling D. Functional analysis of mutations in the gamma 2 subunit of AMP-activated protein kinase associated with cardiac hypertrophy and Wolff-Parkinson-White syndrome. J Biol Chem 2002;277:51017–24. [PubMed: 12397075]
10. Luptak I, Shen M, He H, Hirshman MF, Musi N, Goodyear LJ, et al. Aberrant activation of AMP-activated protein kinase remodels metabolic network in favor of cardiac glycogen storage. The Journal of clinical investigation 2007;117:1432–9. [PubMed: 17431505]
11. Wright EM, Loo DD, Panayotova-Heiermann M, Lostao MP, Hirayama BH, Mackenzie B, et al. 'Active' sugar transport in eukaryotes. J Exp Biol 1994;196:197–212. [PubMed: 7823022]
12. Schwenk RW, Luiken JJ, Bonen A, Glatz JF. Regulation of sarcolemmal glucose and fatty acid transporters in cardiac disease. Cardiovasc Res 2008;79:249–58. [PubMed: 18469026]
13. Banerjee SK, McGaffin KR, Pastor-Soler NM, Ahmad F. SGLT1 is a novel cardiac glucose transporter that is perturbed in disease states. Cardiovasc Res 2009;84:111–8. [PubMed: 19509029]
14. Banerjee SK, McGaffin KR, Huang XN, Ahmad F. Activation of cardiac hypertrophic signaling pathways in a transgenic mouse with the human PRKAG2 Thr400Asn mutation. Biochim Biophys Acta. 2009
15. Xing Y, Musi N, Fujii N, Zou L, Luptak I, Hirshman MF, et al. Glucose metabolism and energy homeostasis in mouse hearts overexpressing dominant negative alpha2 subunit of AMP-activated protein kinase. J Biol Chem 2003;278:28372–7. [PubMed: 12766162]
16. McGaffin KR, Sun CK, Rager JJ, Romano LC, Zou B, Mathier MA, et al. Leptin signalling reduces the severity of cardiac dysfunction and remodelling after chronic ischaemic injury. Cardiovasc Res 2008;77:54–63. [PubMed: 18006469]
17. Ahmad F, Banerjee SK, Lage ML, Huang XN, Smith SH, Saba S, et al. The role of cardiac troponin T quantity and function in cardiac development and dilated cardiomyopathy. PLoS ONE 2008;3:e2642. [PubMed: 18612386]
18. Pastor-Soler NM, Hallows KR, Smolak C, Gong F, Brown D, Breton S. Alkaline pH- and cAMP-induced V-ATPase membrane accumulation is mediated by protein kinase A in epididymal clear cells. Am J Physiol Cell Physiol 2008;294:C488–94. [PubMed: 18160485]

19. Breton S, Tyszkowski R, Sabolic I, Brown D. Postnatal development of H+ ATPase (proton-pump)-rich cells in rat epididymis. Histochemistry and cell biology 1999;111:97–105. [PubMed: 10090570]
20. Brown D, Lydon J, McLaughlin M, Stuart-Tilley A, Tyszkowski R, Alper S. Antigen retrieval in cryostat tissue sections and cultured cells by treatment with sodium dodecyl sulfate (SDS). Histochemistry and cell biology 1996;105:261–7. [PubMed: 9072183]
21. Pastor-Soler N, Bagnis C, Sabolic I, Tyszkowski R, McKee M, Van Hoek A, et al. Aquaporin 9 expression along the male reproductive tract. Biology of reproduction 2001;65:384–93. [PubMed: 11466204]
22. Blahnik KR, Dou L, O'Geen H, McPhillips T, Xu X, Cao AR, et al. Sole-Search: an integrated analysis program for peak detection and functional annotation using ChIP-seq data. Nucleic Acids Res 38:e13. [PubMed: 19906703]
23. Young LH, Renfu Y, Russell R, Hu X, Caplan M, Ren J, et al. Low-flow ischemia leads to translocation of canine heart GLUT-4 and GLUT-1 glucose transporters to the sarcolemma in vivo. Circulation 1997;95:415–22. [PubMed: 9008459]
24. Tian R, Musi N, D'Agostino J, Hirshman MF, Goodyear LJ. Increased adenosine monophosphate-activated protein kinase activity in rat hearts with pressure-overload hypertrophy. Circulation 2001;104:1664–9. [PubMed: 11581146]
25. Broderick TL, King TM. Upregulation of GLUT-4 in right ventricle of rats with monocrotaline-induced pulmonary hypertension. Med Sci Monit 2008;14:BR261–4. [PubMed: 19043358]
26. Russell RR 3rd, Li J, Coven DL, Pypaert M, Zechner C, Palmeri M, et al. AMP- activated protein kinase mediates ischemic glucose uptake and prevents postischemic cardiac dysfunction, apoptosis, and injury. The Journal of clinical investigation 2004;114:495–503. [PubMed: 15314686]
27. Li J, Miller EJ, Ninomiya-Tsuji J, Russell RR 3rd, Young LH. AMP-activated protein kinase activates p38 mitogen-activated protein kinase by increasing recruitment of p38 MAPK to TAB1 in the ischemic heart. Circ Res 2005;97:872–9. [PubMed: 16179588]
28. Martin MG, Wang J, Solorzano-Vargas RS, Lam JT, Turk E, Wright EM. Regulation of the human Na(+)-glucose cotransporter gene, SGLT1, by HNF-1 and Sp1. Am J Physiol Gastrointest Liver Physiol 2000;278:G591–603. [PubMed: 10762614]
29. Nilsson EC, Long YC, Martinsson S, Glund S, Garcia-Roves P, Svensson LT, et al. Opposite transcriptional regulation in skeletal muscle of AMP-activated protein kinase gamma3 R225Q transgenic versus knock-out mice. J Biol Chem 2006;281:7244–52. [PubMed: 16410251]
30. Hedegaard J, Horn P, Lametsch R, Sondergaard Moller H, Roepstorff P, Bendixen C, et al. UDP-glucose pyrophosphorylase is upregulated in carriers of the porcine RN- mutation in the AMP-activated protein kinase. Proteomics 2004;4:2448–54. [PubMed: 15274139]
31. Russell RR 3rd, Bergeron R, Shulman GI, Young LH. Translocation of myocardial GLUT-4 and increased glucose uptake through activation of AMPK by AICAR. Am J Physiol 1999;277:H643–9. [PubMed: 10444490]
32. Zhou L, Cryan EV, D'Andrea MR, Belkowski S, Conway BR, Demarest KT. Human cardiomyocytes express high level of Na+/glucose cotransporter 1 (SGLT1). J Cell Biochem 2003;90:339–46. [PubMed: 14505350]
33. Turk E, Kerner CJ, Lostao MP, Wright EM. Membrane topology of the human Na+/glucose cotransporter SGLT1. J Biol Chem 1996;271:1925–34. [PubMed: 8567640]
34. Loo DD, Hirayama BA, Sala-Rabanal M, Wright EM. How drugs interact with transporters: SGLT1 as a model. J Membr Biol 2008;223:87–106. [PubMed: 18592293]
35. Turk E, Martin MG, Wright EM. Structure of the human Na+/glucose cotransporter gene SGLT1. J Biol Chem 1994;269:15204–9. [PubMed: 8195156]
36. Turk E, Klisak I, Bacallao R, Sparkes RS, Wright EM. Assignment of the human Na+/glucose cotransporter gene SGLT1 to chromosome 22q13.1. Genomics 1993;17:752–4. [PubMed: 8244393]
37. Vayro S, Wood IS, Dyer J, Shirazi-Beechey SP. Transcriptional regulation of the ovine intestinal Na+/glucose cotransporter SGLT1 gene. Role of HNF-1 in glucose activation of promoter function. Eur J Biochem 2001;268:5460–70. [PubMed: 11606209]
38. Solomon SS, Majumdar G, Martinez-Hernandez A, Raghow R. A critical role of Sp1 transcription factor in regulating gene expression in response to insulin and other hormones. Life Sci 2008;83:305–12. [PubMed: 18664368]

39. Hirsch JR, Loo DD, Wright EM. Regulation of Na+/glucose cotransporter expression by protein kinases in Xenopus laevis oocytes. J Biol Chem 1996;271:14740–6. [PubMed: 8663046]
40. Wright EM, Hirsch JR, Loo DD, Zampighi GA. Regulation of Na+/glucose cotransporters. J Exp Biol 1997;200:287–93. [PubMed: 9050236]
41. Khoursandi S, Scharlau D, Herter P, Kuhnen C, Martin D, Kinne RK, et al. Different modes of sodium-D-glucose cotransporter-mediated D-glucose uptake regulation in Caco-2 cells. Am J Physiol Cell Physiol 2004;287:C1041–7. [PubMed: 15201142]
42. Kipp H, Khoursandi S, Scharlau D, Kinne RK. More than apical: Distribution of SGLT1 in Caco-2 cells. Am J Physiol Cell Physiol 2003;285:C737–49. [PubMed: 12773314]
43. Ehrenkranz JR, Lewis NG, Kahn CR, Roth J. Phlorizin: a review. Diabetes Metab Res Rev 2005;21:31–8. [PubMed: 15624123]
44. Pajor AM, Randolph KM, Kerner SA, Smith CD. Inhibitor binding in the human renal low- and high-affinity Na+/glucose cotransporters. J Pharmacol Exp Ther 2008;324:985–91. [PubMed: 18063724]
45. Kutner S, Breuer WV, Ginsburg H, Cabantchik ZI. On the mode of action of phlorizin as an antimalarial agent in in vitro cultures of Plasmodium falciparum. Biochem Pharmacol 1987;36:123–9. [PubMed: 3099799]
46. Minokoshi Y, Kim YB, Peroni OD, Fryer LG, Muller C, Carling D, et al. Leptin stimulates fatty-acid oxidation by activating AMP-activated protein kinase. Nature 2002;415:339–43. [PubMed: 11797013]
47. Kimura Y, Turner JR, Braasch DA, Buddington RK. Lumenal adenosine and AMP rapidly increase glucose transport by intact small intestine. Am J Physiol Gastrointest Liver Physiol 2005;289:G1007–14. [PubMed: 16020657]
48. Sopjani M, Bhavsar SK, Fraser S, Kemp BE, Foller M, Lang F. Regulation of Na+-coupled glucose carrier SGLT1 by AMP-activated protein kinase. Mol Membr Biol 27:137–44. [PubMed: 20334581]
49. Walker J, Jijon HB, Diaz H, Salehi P, Churchill T, Madsen KL. 5-aminoimidazole-4-carboxamide riboside (AICAR) enhances GLUT2-dependent jejunal glucose transport: a possible role for AMPK. Biochem J 2005;385:485–91. [PubMed: 15367103]
50. Tan NY, Khachigian LM. Sp1 phosphorylation and its regulation of gene transcription. Mol Cell Biol 2009;29:2483–8. [PubMed: 19273606]
51. Jakobsen SN, Hardie DG, Morrice N, Tornqvist HE. 5'-AMP-activated protein kinase phosphorylates IRS-1 on Ser-789 in mouse C2C12 myotubes in response to 5-aminoimidazole-4-carboxamide riboside. J Biol Chem 2001;276:46912–6. [PubMed: 11598104]
52. Kawano K, Ikari A, Nakano M, Suketa Y. Phosphatidylinositol 3-kinase mediates inhibitory effect of angiotensin II on sodium/glucose cotransporter in renal epithelial cells. Life Sci 2002;71:1–13. [PubMed: 12020744]
53. Loflin P, Lever JE. HuR binds a cyclic nucleotide-dependent, stabilizing domain in the 3' untranslated region of Na(+)/glucose cotransporter (SGLT1) mRNA. FEBS Lett 2001;509:267–71. [PubMed: 11741601]
54. Martinez-Chantar ML, Vazquez-Chantada M, Garnacho M, Latasa MU, Varela-Rey M, Dotor J, et al. S-adenosylmethionine regulates cytoplasmic HuR via AMP-activated kinase. Gastroenterology 2006;131:223–32. [PubMed: 16831604]
55. Balakrishnan A, Stearns AT, Rounds J, Irani J, Giuffrida M, Rhoads DB, et al. Diurnal rhythmicity in glucose uptake is mediated by temporal periodicity in the expression of the sodium-glucose cotransporter (SGLT1). Surgery 2008;143:813–8. [PubMed: 18549898]
56. Stearns AT, Balakrishnan A, Rhoads DB, Ashley SW, Tavakkolizadeh A. Diurnal expression of the rat intestinal sodium-glucose cotransporter 1 (SGLT1) is independent of local luminal factors. Surgery 2009;145:294–302. [PubMed: 19231582]
57. Ahmad F, Seidman JG, Seidman CE. The genetic basis for cardiac remodeling. Annu Rev Genomics Hum Genet 2005;6:185–216. [PubMed: 16124859]

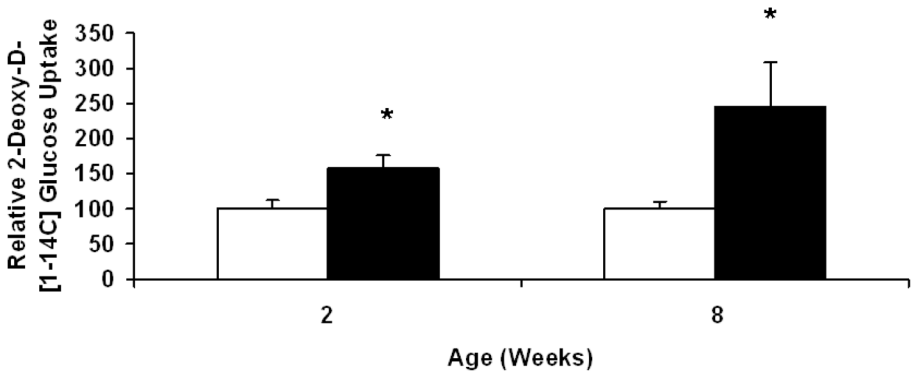

Fig. 1.

Cardiac glucose uptake was increased in TG^{T400N} mice relative to WT littermates at ages 2 and 8 weeks, as assessed by administration of 2-deoxy-D-[1-14C] glucose (2-[14C]DG) (10 μCi) IP. Open bars, WT; closed bars, TG^{T400N}. $n = 3$ / group. *, $P<0.05$ versus WT.

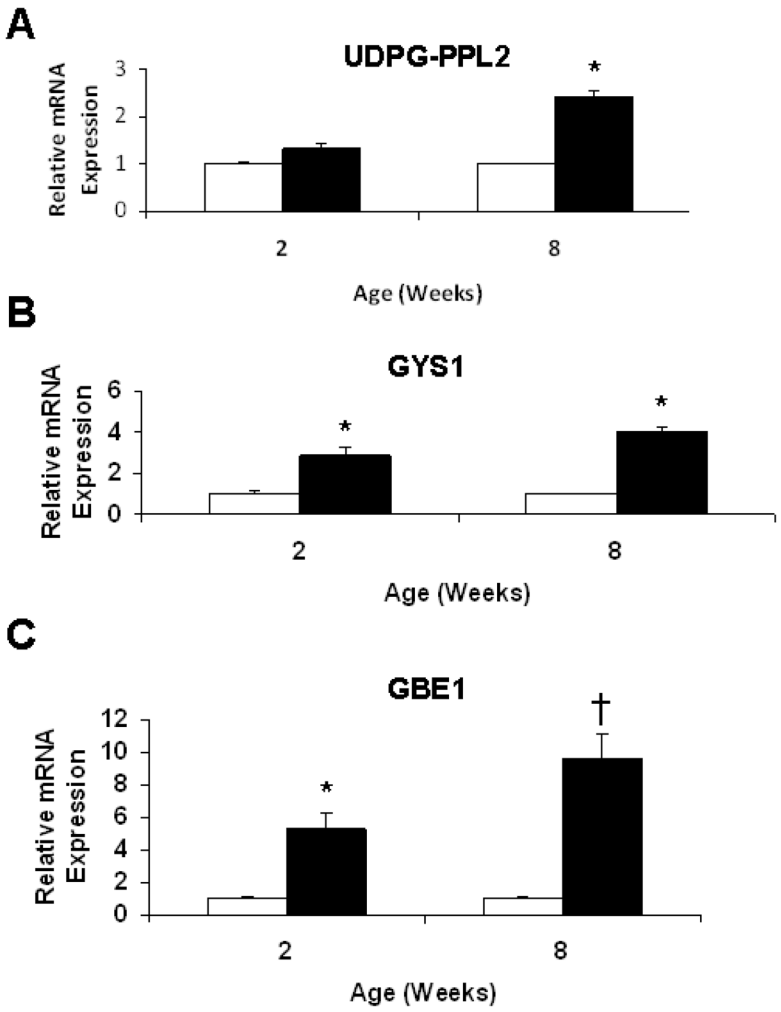

Fig. 2.

mRNA expression of genes responsible for glycogen synthesis was measured by real-time quantitative PCR (QPCR) in total cardiac tissue from TG^{T400N} mice and WT littermates at ages 2 and 8 weeks. (A) UDP glucose pyrophosphorylase 2 (UDPG-PPL2) transcript levels were significantly increased in TG^{T400N} hearts at age 8 weeks, but not at age 2 weeks. (B) Glycogen synthase 1 (GYS1) and (C) glucan branching 1 (GBE1) transcript levels were significantly increased in TG^{T400N} hearts at ages 2 and 8 weeks. Open bars, WT; closed bars, TG^{T400N}. $n = 3$ / group. *, $P<0.05$; †, $P<0.01$ versus WT.

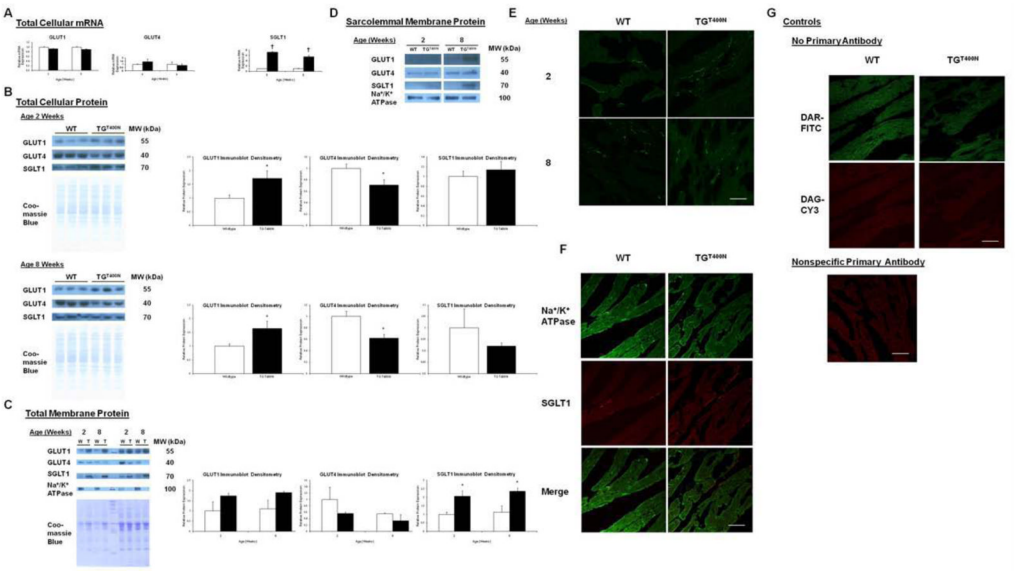

Fig. 3.

Cardiac GLUT1, GLUT4, and SGLT1 mRNA and protein expression in TG^{T400N} mice. (A) Total cardiac GLUT1 and GLUT4 transcript expression, as assessed by QPCR, were similar in TG^{T400N} mice and WT littermates at ages 2 and 8 weeks, whereas cardiac SGLT1 transcript expression was increased in TG^{T400N} mice at ages 2 and 8 weeks ($n = 3$ / group). (B) In whole heart homogenates, densitometry analysis of immunoblots showed that GLUT1 protein was significantly increased, GLUT4 protein was significantly decreased, and SGLT1 protein was unchanged in TG^{T400N} mice relative to WT littermates at ages 2 and 8 weeks. (C) In total membrane extracts, densitometry analysis of immunoblots showed that GLUT1 and GLUT4 protein expression was not significantly different in TG^{T400N} mice relative to WT littermates at ages 2 and 8 weeks, whereas SGLT1 protein expression was significantly increased in TG^{T400N} mice at ages 2 and 8 weeks. (D) In sarcolemmal membrane extracts, GLUT1 and SGLT1 protein expression appeared to be mildly increased at age 2 weeks and greatly increased at age 8 weeks in TG^{T400N} mice relative to WT littermates, whereas there was no apparent difference in GLUT4 expression ($n = 10 - 12$ / group, pooled into one lane). The α1 subunit of the Na^+/K^+-ATPase, a sarcolemmal membrane marker, was used to document adequate enrichment of membrane fractions. (E)Immunofluorescence microscopy showed that SGLT1 (green) had similar subcellular distributions in WT and TG^{T400N} cardiac myocytes at ages 2 and 8 weeks. (F) Immunofluorescence microscopy showed that α-subunit Na^+/K^+-ATPase (green, upper panel) and SGLT1 (red, middle panel) partially co-localized (lower panel) with in cardiac myocytes from 8 week old WT and TG^{T400N} mice. (G) Control incubations were performed with secondary antibody only (“no-primary” control) and with nonspecific primary antibody, and showed no immunofluorescence labeling under identical acquisition conditions. Open bars, WT; closed bars, TG^{T400N}. T, TG^{T400N}; W, WT. Molecular weights (MW) on immunoblots were estimated by protein marker sizes. Coomassie blue staining was used to document the relative quantity of protein loaded for the immunoblots and to normalize densitometry analysis. Scale bars on photomicrographs represent 37.5 μm. *, $P<0.05$; †, $P<0.01$ versus WT.

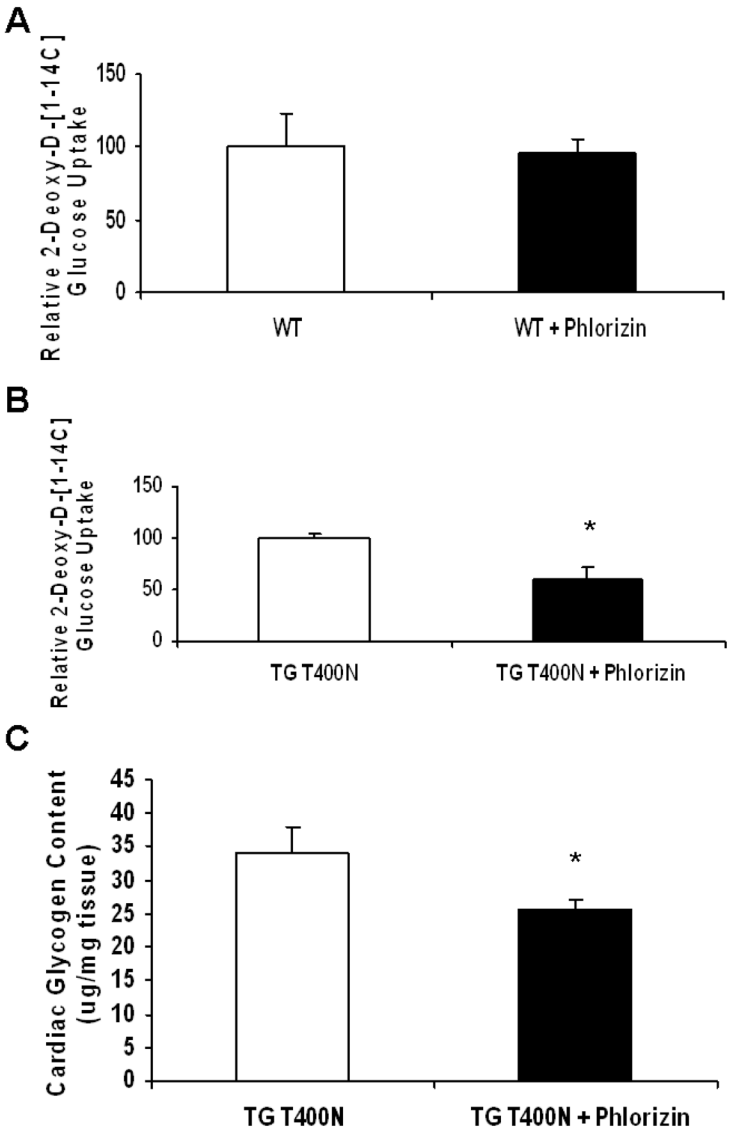

Fig. 4.

Increased cardiac glucose uptake and glycogen deposition in TG^{T400N} mice was sensitive to phlorizin, a specific SGLT1 inhibitor. (A) There was no significant change in cardiac glucose uptake in 6–8 week old WT mice 10 min following acute administration of phlorizin (400 mg/kg IP). (B) In contrast, cardiac glucose uptake was reduced in 6–8 week old TG^{T400N} mice 10 min following acute administration of phlorizin (400 mg/kg IP). (C) Chronic administration phlorizin (100 mg/kg/day) using a subcutaneous osmotic minipump in TG^{T400N} mice from age 2 weeks through age 6 weeks resulted in a reduction in cardiac glycogen content. Open bars, vehicle treated control mice; closed bars, phlorizin treated mice. $n = 4$ / group, *, $P<0.05$ relative to control.

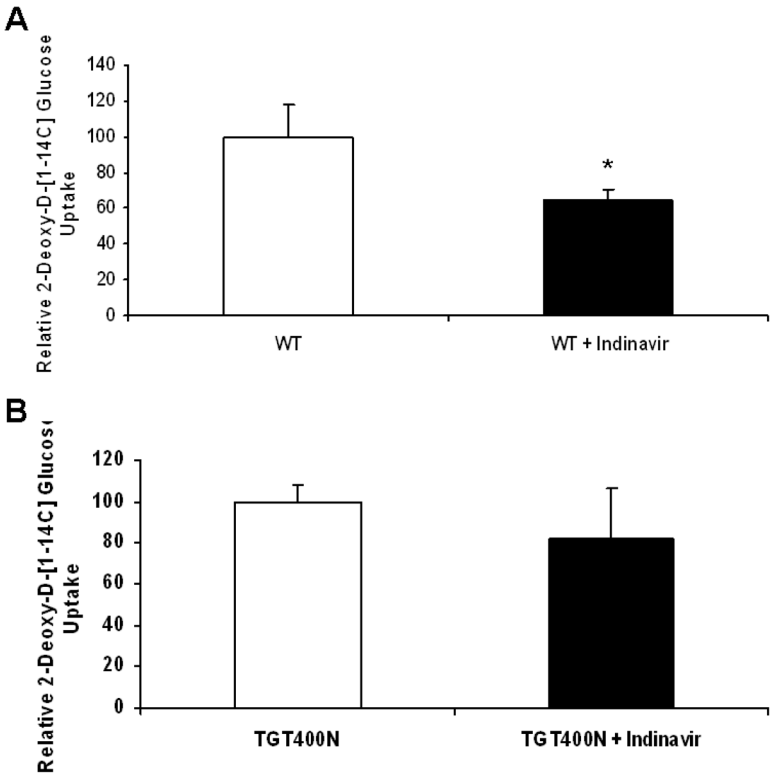

Fig. 5.

Increased cardiac glucose uptake in TG^{T400N} mice was not significantly sensitive to indinavir, a GLUT inhibitor. (A) There was a significant change in cardiac glucose uptake in 6–8 week old WT mice 10 min following acute administration of indinavir (10mg/kg IP). (B) In contrast, cardiac glucose uptake was not significantly reduced in 6–8 week old TG^{T400N} mice 10 min following acute administration of indinavir (10 mg/kg IP). Open bars, vehicle treated control mice; closed bars, indinavir treated mice. $n = 4$ / group, *, $P<0.05$ relative to control.

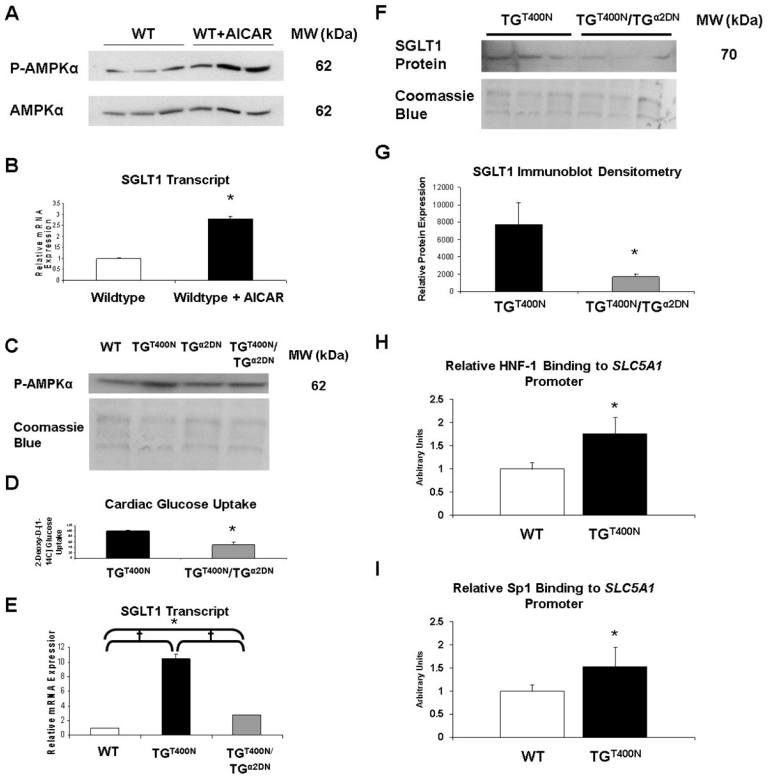

Fig. 6.

Cardiac SGLT1 expression was regulated by AMPK. (A) Levels of Thr^{172} phosphorylated AMPK a subunit (P-AMPKα), which reflect AMPK activity, were increased in 8 week old male WT FVB mice after administration of the AMPK activator AICAR (500 μg/kg IP, twice at a 3 h interval). (B) Concurrently, cardiac SGLT1 mRNA expression was increased in these mice after administration of AICAR (n = 6 / group). (C) Levels of Thr^{172} phosphorylated AMPK α subunit (P-AMPKα) were normalized in $TG^{T400N}/TG^{\alpha 2DN}$ relative to TG^{T400N} hearts at age 2 weeks. (D) Double transgenic mice ($TG^{T400N}/TG^{\alpha 2DN}$) exhibited attenuation of cardiac glucose uptake (n = 3 / group). (E) Increased SGLT1 mRNA expression in TG^{T00N} hearts was attenuated in $TG^{T400N}/TG^{\alpha 2DN}$ hearts, as assessed by QPCR (n = 3 / group). (F) An immunoblot showed that the increased SGLT1 protein expression observed in TG^{T00N} hearts was attenuated in $TG^{T400N}/TG^{\alpha 2DN}$ hearts. (G) Densitometry analysis of the immunoblot shown in panel F. Chromatin immunoprecipitation (ChIP) showed that increased expression of SGLT1 in TG ^{T00N} hearts relative to WT was associated with increased binding of (H) HNF-1 and (I) Sp1 to the promoter of the *SLC5A1* gene encoding SGLT1 (n = 3 / group). Molecular weights (MW) on immunoblots were estimated by protein marker sizes. Coomassie blue staining was used to document the relative quantity of protein loaded for the immunoblots. *, $P<0.05$, †, $P<0.01$.

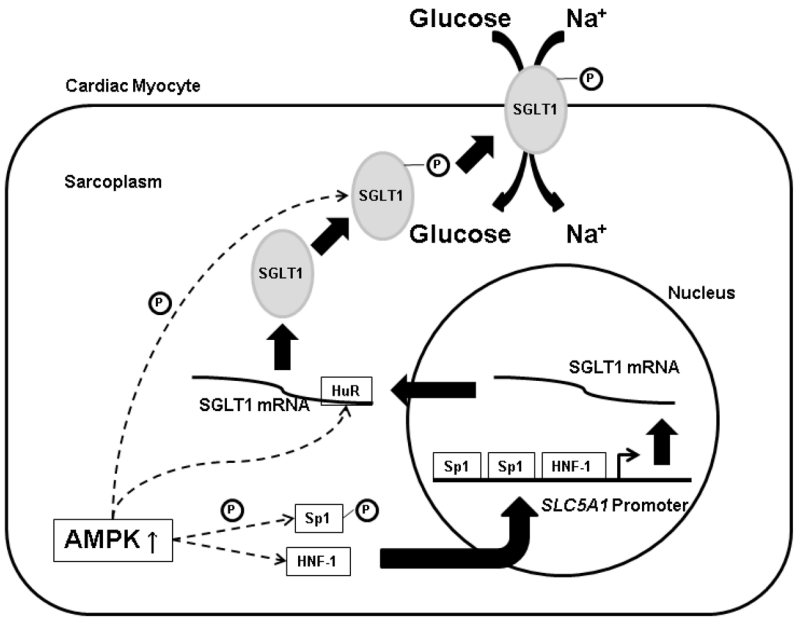

Fig. 7.

A hypothetical model of the mechanism by which increased AMPK activity leads to increased cardiac glucose uptake via SGLT1 in *PRKAG2* cardiomyopathy. AMPK directly or indirectly phosphorylates the transcription factor Sp1, which increases binding of Sp1 to the promoter of the *SLC5A1* gene encoding SGLT. Binding of the transcription factor HNF-1 is also increased by unknown mechanisms. These factors increase transcription of *SLC5A1* . AMPK stimulates binding of the protein HuR to a critical uridine-rich element (URE) in the 3' untranslated region of the SGLT1 transcript, increasing its stability. AMPK directly or indirectly phosphorylates the translated SGLT1 protein, increasing translocation of SGLT1 to the sarcolemma. Increased sarcolemmal SGLT1 then leads to increased cardiac glucose uptake.

Table

Real-time quantitative PCR (QPCR) primers used to quantify mRNA expression and to quantify protein-DNA interaction following chromatin immunoprecipitation.

Cyclophilin	Sense	5’-TGTGCCAGGGTGGTGACTT-3’
	Antisense	5’-TCAAATTTCTCTCCGTAGATGGACTT-3’
GBE1	Sense	5’-CAGGCATGATTATTTTGGCTGT-3’
	Antisense	5’-AATGCAAAGTGAGGCACAGAT-3’
GLUT1	Sense	5’-GAGTGACGATCTGAGCTACGG-3’
	Antisense	5’-CGTTACTCACCTTGCTGCTG-3’
GLUT4	Sense	5’-GTAACTTCATTGTCGGCATGG-3’
	Antisense	5’-CCTGCTCTAAAAGGGAAGGTG-3’
GYS1	Sense	5’-GAATGGCAGTGAGCAAACAGT-3’
	Antisense	5’-TCCTTGTCCAGCATCTTGTTC-3’
HNF-1	Sense	5’-CAGAACAGACTTTACCTGCCG-3’
	Antisense	5’-GCGACAGTGGGGCTGC-3’
SGLT1	Sense	5’-TCTGTAGTGGCAAGGGGAAG-3’
	Antisense	5’-ACAGGGCTTCTGTGTCTTGG-3’
Sp1	Sense	5’-CAGAACAGACTTTACCTGCCG-3’
	Antisense	5’-GCGACAGTGGGGCTGC-3’
UDPG-PPL2	Sense	5’-GAAGATTCGATTCAACCCTAT-3’
	Antisense	5’-AAGGTGTAGATTTTCACACGA-3’